Biased diffusion in anisotropic disordered systems

S. Bustingorry* and E. R. Reyes†
Departamento de Física, Universidad Nacional del Comahue, 8300 Neuquén, Argentina

Manuel O. Cáceres‡
Centro Atómico Bariloche and Instituto Balseiro, CNEA and Universidad Nacional de Cuyo, 8400, Bariloche, Argentina

(Received 9 June 2000)

We investigate a diffusion process into an anisotropic disordered medium in the presence of a bias. The medium is modeled by a two-dimensional square lattice in which the anisotropic disorder is represented by a bond percolation model with different occupation probabilities on each direction. The biased diffusion process is mapped by a random walk with unequal transition probabilities along and against the field (in the [1,1] direction) by performing Monte Carlo simulations. We observe a transition from pure to drift diffusion when the bias reaches a threshold B_c. In order to estimate this B_c, an *effective exponent* is used to characterize the diffusion process. This B_c is also compared with another estimation for the critical field.

PACS number(s): 02.50.Ng, 66.30.−h, 05.40.−a

I. INTRODUCTION

Classical diffusion on disordered systems is a subject of great interest and has been intensively studied in the past two decades [1,2]. In the pioneering work of de Gennes [3], the diffusion of a particle on a percolating lattice, performing a random walk (RW), was called the ant in the labyrinth problem, because not all lattice sites could be used to perform the RW. In the bond percolation problem, all sites are, in principle, accessible but the lattice is restricted by labeling the bonds which connect two sites as accessible or inaccessible with probability p and $1-p$, respectively [4]. There exists a critical probability (percolation threshold p_c) such that an infinite conducting cluster exists for $p>p_c$ and does not exist for $p<p_c$. It is important to note that the percolation threshold depends on the geometric properties of the lattice and the kind of percolation problem to be studied (site or bond). These models have many applications, including diffusion processes and those related to critical phenomena due to the existence of the characteristic threshold (see Ref. [5] for a general review on percolation). In general, it is possible to characterize the diffusion process by means of a power-law expression for the mean-square displacement (MSD)

$$\langle r^2\rangle \propto t^k. \tag{1}$$

When $k=1$, the process is called normal diffusion, i.e., a RW on an ordered or weak disordered medium. When $k\neq 1$, the process is called anomalous diffusion.

Let us now consider a bias applied in a certain direction of the lattice. An interesting question arises: What is the power-law behavior of the MSD when a bias is switched on, causing the RW to move with unequal probabilities in opposite directions? It is known that for the ordered case and in the long-time regime, $k=2$, but does the walker reach this value on a random medium? This problem [6–10] has been recently revisited [11–13] in an attempt to solve the old controversy of whether or not there exists a transition from drift to no drift for a finite bias [6,7]. This transition occurs from a finite velocity regime to an asymptotic vanishing velocity regime for a characteristic critical external field B_c. The recent theory of Dhar and Stauffer (DS) [11] argues in favor of the existence of a critical field. In this theory, the concept of *trap* generated from the disorder on the cluster is important since these traps act as potential wells and retard notoriously the biased diffusion of the particle, causing the *drift/no-drift* transition. An increase in p increases the connectivity of the cluster resulting in a decrease of the mean depth of traps and, consequently, in an increase in the critical field, i.e., stronger bias is necessary to cause the mean-trapping time to diverge. These arguments are valid for both site and bond percolation model due to the similar shape of the cluster generated.

In order to study this problem, it is convenient to define an *effective exponent* [9]

$$k_{\mathrm{eff}}(t)=\frac{d(\log_{10}\langle r^2\rangle)}{d(\log_{10}t)}, \tag{2}$$

which describes the variation with time of the *effective* power law. Note that this definition is not equivalent to the power law in Eq. (1) with $k=k_{\mathrm{eff}}$. The effective exponent k_{eff} defined in Eq. (2) just represents the rate of variation of $\log_{10}\langle r^2\rangle$ with respect to $\log_{10}(t)$ at time t. The effective exponent accounts for the critical behavior, since it approaches an asymptotic value faster with increasing bias and there exists a characteristic bias B_c above which this approach is retarded on further increasing bias.

Previous studies [9,10,12,14] have dealt with an isotropic medium, and here we are interested in studying the related problem of anisotropic disordered systems, in which not all directions are equivalent. These anisotropic systems are important from an applied point of view. As a matter of fact, in the oil industry, the dielectric properties of reservoir rocks are measured to determine the hydrocarbon content. In this context, water saturation in shaly sandstones can be related to the electric conductivity. The main problem to model the electrical conductivity in the above-mentioned systems arises

*Email address: sbusting@cab.cnea.gov.ar
†Email address: reyes@uncoma.edu.ar
‡Email address: caceres@cab.cnea.gov.ar

because the porous reservoir rocks generally show strong anisotropy, which can be produced by geometrical or intrinsic conductivity factors. This fact has led to an increased focus on the conductivity on an anisotropic rock formation, because the effects of resistivity and induction logging tools are very important for a reliable hydrocarbon saturation evaluation [15]. A second problem that we want to mention here is the analysis of transport in epoxy-graphite disk composites. These are very anisotropic materials due to the intrinsic anisotropic conductivity and preferential orientation upon deposition in the preparation procedures of the sample. The study of dc electric properties, in these composites, as a function of the electric field has inspired recent interest [16].

The aim of our work is to analyze the behavior of a RW on an anisotropic disordered medium under the presence of an external bias, which mimics a particle moving on an anisotropic amorphous material.

II. ANISOTROPIC MODEL

To represent the anisotropic disorder of the system, we consider a bond percolating model on a two-dimensional square lattice with different occupation probabilities on each perpendicular direction. In the x direction (y direction), we keep a bond with probability p_x (p_y) and cut it with probability $1-p_x$ ($1-p_y$). respectively. In the unbiased problem, this kind of system leads, in general, to different diffusion coefficients for each direction [17], and important changes in the biased problem are expected.

Note that in an isotropic percolating medium, there exists a percolation threshold p_c, which for the bond percolation model on a square lattice takes the value $p_c=\frac{1}{2}$. In anisotropic systems this threshold becomes a critical surface of the form $\varphi(p_i,p_j,\ldots)=0$ [18]. For the bond percolation model discussed here, $\varphi(p_x,p_y)=p_x+p_y-1$ [18,19].

Here we performed a RW with unequal transition probabilities along and against the external field. The field is measured by its strength B, being $0\leqslant B<1$. A bias is introduced in the diagonal direction [1,1] of the square lattice. We make this selection because of the privilege introduced in the coordinate system by considering the symmetry of our anisotropic model. Assuming the lattice constant $a=1$, the transition probability $w(\mathbf{r}\rightarrow\mathbf{r}+\delta)$ from $\mathbf{r}$ to $\mathbf{r}+\delta$ is defined as

$$w(\mathbf{r}\rightarrow\mathbf{r}+\delta)=\begin{cases}\frac{1}{4}(1+B) & \text{if } \delta=(1,0) \text{ or } (0,1),\\ \frac{1}{4}(1-B) & \text{if } \delta=(-1,0) \text{ or } (0,-1).\end{cases} \tag{3}$$

Now it is useful to introduce two new parameters p_m and p_d, defined as

$$p_m=\frac{p_x+p_y}{2}, \tag{4}$$

$$p_d=|p_x-p_y|. \tag{5}$$

The first one represents the global occupancy and indicates how far the system is from the percolation threshold $p_x+p_y=1$, where it takes the value $p_{m,c}=\frac{1}{2}$. The second parameter is a measure of the anisotropy of the configuration. When $p_d=0$, we have $p_x=p_y$, i.e., the isotropic case. The general anisotropic case is considered by setting $0<p_d\leqslant p_d^*$, with $p_d^*=2(1-p_m)$. For a fixed p_d, the allowed values of p_m are those lying in the range $p_{m,c}\leqslant p_m\leqslant p_m^*$ with $p_m^*=1-(p_d/2)$. Due to the symmetry of the problem, with respect to $p_x=p_y$, we have worked out only the region $p_x>p_y$, so we can set $p_d=p_x-p_y$.

In the present paper, we work with configurations that are far above the threshold $p_{m,c}$, because near to the formation of the incipient percolation cluster there are a variety of complex phenomena. These problems must be handled with a more sophisticated computer system; the results presented here were just achieved with a PC Pentium III with 500 MHz.

III. RESULTS

A. The effective exponent k_{eff}

We perform Monte Carlo (MC) simulations of the RW in lattices of 500×500 sites with previously selected bond concentrations p_x and p_y, and performed up to 10^6 MC time steps, averaging between 200 and 1000 lattices with 10 walks each. For each configuration (p_x,p_y) we computed the MSD and calculated the effective exponent k_{eff} at various MC time steps. We consider periodic boundary conditions.

First of all, we have compared our MC data, for the isotropic ordered case, with analytical results obtained by using a discrete time RW formalism for the probability of being in site $\mathbf{r}$ at time t [1]; the transition probabilities were defined in Eq. (3). It is then possible to obtain an analytic expression for the MSD and its effective exponent, as a function of the external bias B,

$$\langle r^2\rangle=\frac{(2-B^2)\ t+B^2t^2}{2}, \tag{6}$$

thus

$$k_{\text{eff}}=\frac{(2-B^2)\ t+2\ B^2t^2}{(2-B^2)\ t+B^2t^2}. \tag{7}$$

Note that when $B=0$, we obtain $k_{\text{eff}}(t)=1$ as expected. In addition, for all $B\neq0$ we get $k_{\text{eff}}(t\rightarrow\infty)=2$, i.e., a completely biased particle. In Fig. 1(a), we present the result expressed by Eq. (7) together with our MC data, finding a very good agreement with our simulation. We shall refer to these plots as k_{eff} *plots*.

Second, let us consider a very simple case of anisotropic disordered media: the disorder appears only in one direction (say the y axes). For example, $p_x=1$ and $p_y\neq1$. Although $p_d\neq0$ and $p_m\neq1$ in this special anisotropic case we obtain a *quasiordered* result. This can be seen comparing Figs. 1(a) and 1(b). It is important to remark that in this case $k_{\text{eff}}(t\rightarrow\infty)\rightarrow2$ just as in the completely ordered case, see Eq. (7).

The typical behavior of the effective exponent $k_{\text{eff}}(t)$ for arbitrary values of the occupancy probabilities p_x and p_y (or p_m and p_d) is represented in Fig. 2, for different values of the external field B. Figure 2(a) shows how, at low bias, the exponent increases until it reaches its asymptotic value 2,

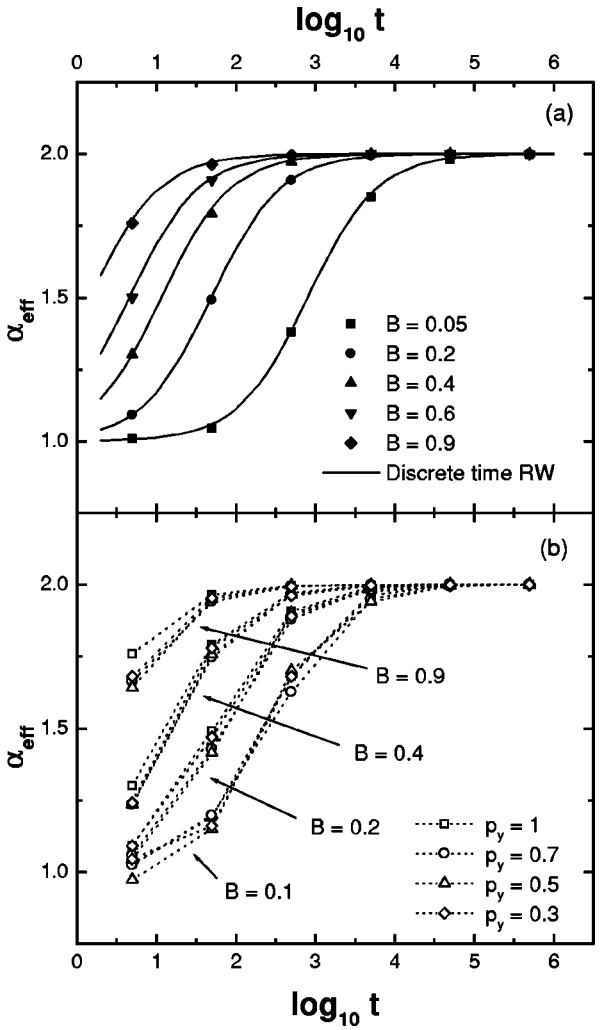

FIG. 1. (a) Monte Carlo data and analytic $k_{\mathrm{eff}}(t)$ from Eq. (7) for the isotropic ordered case ($p_x=1$ and $p_y=1$), for different values of B. (b) $k_{\mathrm{eff}}(t)$ as a function of $\log_{10}(t)$ for $p_x=1$ and p_y $(=1,0.7,0.5,0.3)$ for different values of B. Times are measured in units of diffusion attempts.

reaching this value faster while B increases. Compare, for example, curves with $B=0.1$ and $B=0.2$. It is also possible to realize that there is a characteristic bias B_c, which we associate with a plateau in $k_{\mathrm{eff}}(t)$, above which increasing the bias will cause the exponent $k_{\mathrm{eff}}(t)$ to decrease. This behavior shows, qualitatively, the *drift*/*no-drift* transition which depends on the strength of the external field and the parameters p_m and p_d. We remark that the statistical fluctuations have been averaged in order to obtain B_c. In Figs. 2(b) and 2(c), we show the behavior of $k_{\mathrm{eff}}(t)$ for the same values of B for $p_m=0.525$ and p_d $(=0.05,0.35)$, respectively. Figures 2(a), 2(c), and 2(d) are k_{eff} plots for the same value of p_x but different values of p_y.

Finally, we point out that we have found a characteristic oscillatory behavior of the effective exponent for bias fields far above the critical value B_c, which is not studied here. In this range, the exponent $k_{\mathrm{eff}}(t)$ presents a log-periodic variation due to the discrete-scale invariance of the cluster related to the depth distribution of traps [13,14,20]. These effects are present in our simulations but it is still difficult, with our MC simulations, to take into account the role of anisotropy.

B. Dhar and Sttaufer estimation of B_c

As mentioned before in the Introduction, DS [11] worked out a theory for the *drift*/*no-drift* transition. The main ingredient of such a theory is the depth distribution of traps $P(l)$. When a particle gets into a trap of depth l, it has to do l steps against the bias to get out and continue diffusing. As suggested earlier [7,8], this depth has an exponential distribution $P(l)\propto\exp(-A\ l)$, where the parameter A is an unknown p-dependent function. With this condition, DS derived an expression for the critical bias B_c, at which the time spent by the RW in the trap diverges $\langle\tau\rangle=\Sigma_{l=0}^{\infty}\tau_l P(l)$, where τ_l is the time spent at a trap of depth l. Using the exponential decay for the depth distribution, they showed that at $B=B_c$, the average velocity at large t decreases to zero as $1/\log_{10}(t)$.

Our anisotropic bond percolation model has the same kind of geometric properties as in the DS isotropic site percolation model, the main difference being the change in morphology of the resulting cluster. This allows us the use of an exponential decay for the depth distribution of traps but with a modified unknown parameter $A^{\mathrm{ani}}(p_m,p_d)$, containing all the information of the new cluster morphology. For our *bond* model, $A^{\mathrm{ani}}(p_m,p_d=0)=A^{\mathrm{iso}}(p_m)$, which still differs from the *site* model used by DS [11] and Kirsch [12,21]. In this way, we argue that all the arguments developed by DS are also valid for our model but taking A^{ani} as the exponential parameter. Thus we can obtain a measure of B_c from the change of the concavity of the reciprocal velocity $1/v$ versus $\log_{10}(t)$ (DS plots) at various B, as was proposed by DS. We then used these values to compare with our previous k_{eff} estimations.

In Fig. 3, we present a phase diagram of B_c versus p_m for various p_d values obtained from DS plots. The value $B_c\to 1$ when $p_m\to p_m^*=1-(p_d/2)$ is an extrapolation of nonnumerical results. This limit can be thought of by considering that when the global occupancy increases, the depth of the traps gets smaller and smaller reaching, finally, a quasiordered behavior when there is no trap. On the other hand, we know that the smaller the depth is, the larger the field B_c must be in order to stack the particle into the traps, i.e., $p_m\to p_m^*$. Thus in the particular situation $p_m\to p_m^*$, the characteristic field tends to its maximum value, i.e., $B_c\to 1$. The inset of Fig. 3 shows the phase diagram of B_c versus p_d at constant p_m.

Furthermore, we can adapt the formula used by DS [relating B_c and $A^{ani}(p_m,p_d)$] to our anisotropic bond percolation problem, which yields

$$\frac{1+B_c}{1-B_c}=\exp[A^{\mathrm{ani}}(p_m,p_d)]. \tag{8}$$

From our B_c versus p_m data, Fig. 3, and applying Eq. (8) we obtain the variation of the exponential parameter $A^{\mathrm{ani}}(p_m,p_d)$ with the anisotropy; this is plotted in Fig. 4. This figure gives support to our conjecture of using Eq. (8) even in the anisotropic case. This is insinuated in Fig. 4, where for a fixed p_d, when $p_m\to p_m^*$, the tendency of A^{ani} shows a divergency at $p_m^*(p_d)$. This fact can heuristically be understood from the calculation of the mean-trapping time as a function of the global occupancy $\langle\tau\rangle\sim\Sigma_{l=0}^{\infty}\{(1+B)/[(1$

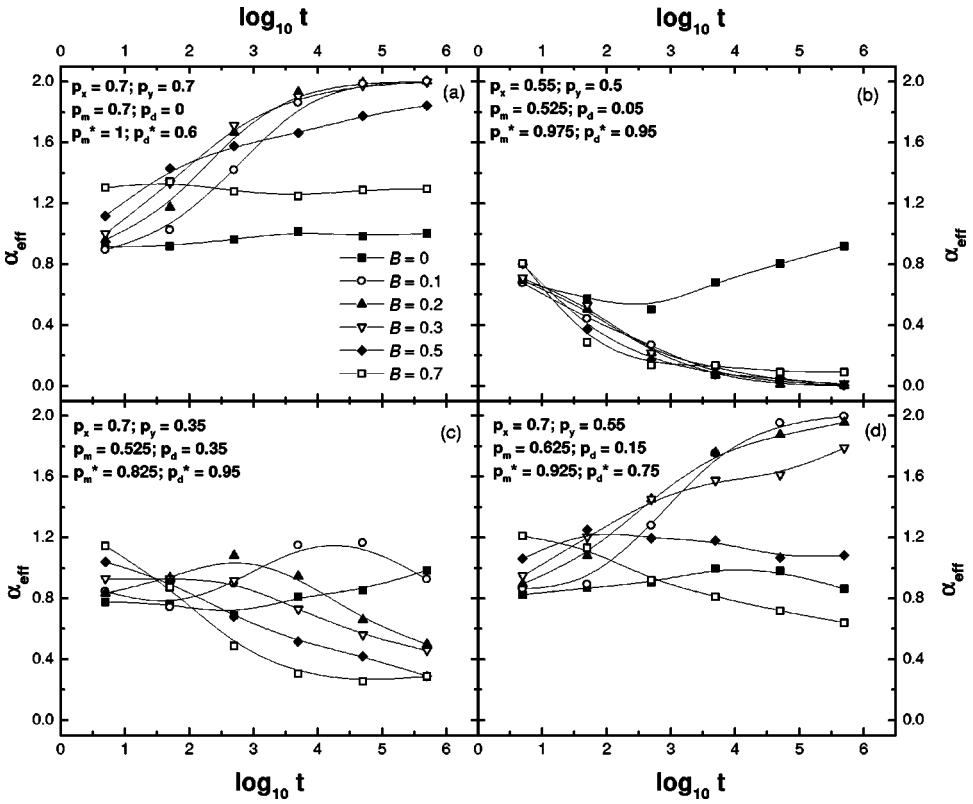

FIG. 2. $k_{\mathrm{eff}}(t)$ plots for various values of p_x and p_y (or p_m and p_d). The strength of the bias B in (b), (c), and (d) is the same as in (a). The corresponding values of p_d^* and p_m^*, for each case, are also shown. The lines are only guides to the eye. Time units as in Fig. 1.

$-B)e^{A^{\mathrm{ani}}}]\}^l$. For $p_m \to p_m^*$, we expect a quasiordered situation (see Fig. 1), so $\langle \tau \rangle \to 0$ because there is no trap. Therefore, $A^{\mathrm{ani}}(p_m \to p_m^*, p_d)$ must diverge in this limit. Indeed this conjecture is compatible with the fact that for $p_m \to p_m^*$ the critical field B_c goes to 1 and $(1-B_c)e^{A^{\mathrm{ani}}} \to \infty$.

IV. DISCUSSION

A. Comparison between k_{eff} and DS estimation of B_c

From the k_{eff} *plots* a value of B_c may be estimated as the bias B for which the effective exponent begins to decrease in time. In Fig. 5, we compare B_c estimations obtained from

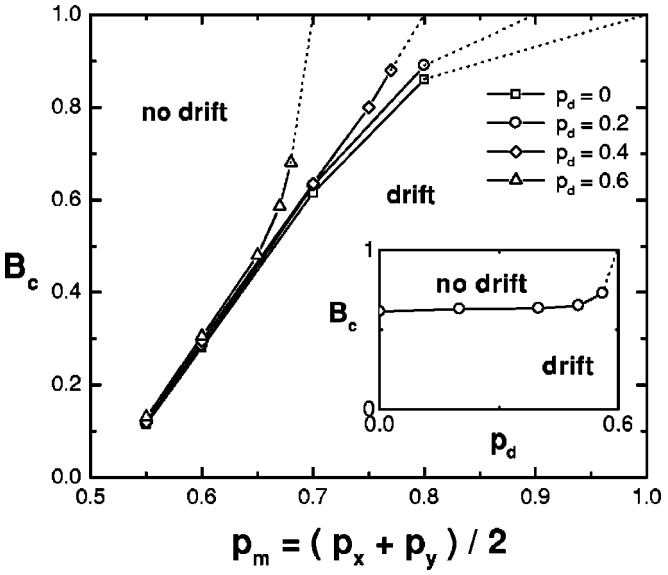

FIG. 3. Phase diagram of B_c versus p_m for different values of p_d. Below each curve we can define the drift regime ($v \neq 0$) and above it the no-drift regime ($v = 0$). See the inset where we show the phase diagram B_c versus p_d (for fixed p_m). The dotted lines are plotted in order to see the corresponding ending points at p_m^* ($=0.7$ for triangles, 0.8 for diamonds, 0.9 for circles, and 1 for squares); and $p_d^* = 0.6$ in the inset. In all points the error bar is about $\Delta B_c = 0.2$.

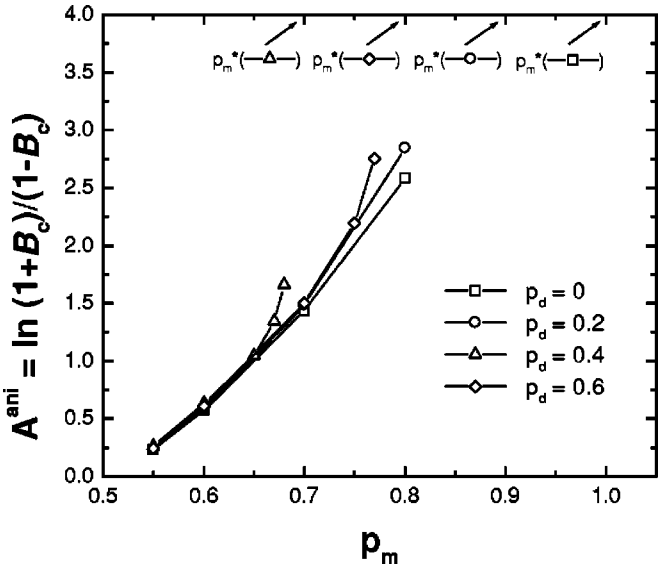

FIG. 4. Exponential parameter A^{ani} versus p_m for different p_d. Some of the curves show the behavior of $A^{\mathrm{ani}}(p_m)$ when p_m goes to p_m^*. It can be seen that the curves asymptotically diverge at p_m^*. At least there is an insinuation for triangles and diamonds. For circles and squares, where we expect higher values of B_c, the log-periodic oscillations shadow this asymptotic behavior, so we cannot go to these higher values of B_c. A^{ani} is measured in units of $1/a$, where a is the lattice constant.

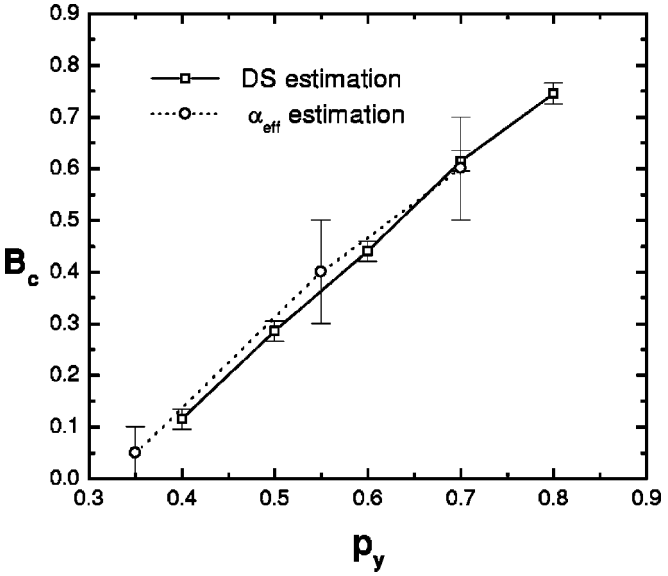

FIG. 5. Comparison of k_{eff} and DS approaches for the estimation of the critical bias B_c. The plot corresponds to a fixed value of $p_x = 0.7$.

Figs. 2(a), 2(c), and 2(d) (open circles) against estimations from DS plots (open squares), at constant p_x. We find a very good agreement, giving support to both approaches. In both estimates the values could be improved by taking more MC steps and more computer time, but the essential behavior does not change.

Although the values of the critical bias B_c from effective exponent plots do not *demonstrate* the drift/no-drift transition, both approximations seem to be valid. Then, for a given system, we have used two different methods to get the critical bias. One approach is obtained in terms of the behavior of the velocity, or the mean displacement $\langle r(t)\rangle$, as a function of time for various values of the external field. In the second approach, we study the dependency of the effective exponent $k_{\text{eff}}(t)$ as a function of time, or the mean-square displacement $\langle r^2(t)\rangle$, for various external fields *B*.

B. Anisotropic effects

Let us first consider $p_x = 1$, see Fig. 1(b). This behavior can be explained considering that the bias is oriented in the diagonal direction, so there is always an external field acting on the transition probability in all directions. Therefore, when one direction is completely connected, the particle can always be pushed by the bias, as in the completely ordered case ($p_x = 1$ and $p_y = 1$). This means that there are not *dead ends* on the percolating cluster, which would slow down, at any instant, the movement of the RW. This explains why, when $B \neq 0$, $k_{\text{eff}}(t \to \infty)$ takes the value 2 for all p_y, as in the ordered case, see Eq. (7). We would find the same behavior when $p_x \neq 1$ and $p_y = 1$ due to symmetrical properties.

From Figs. 2(b) and 2(c) it is clear that the critical bias B_c grows when p_d is increased and p_m is kept constant. This can also be seen in the inset in Fig. 3. When $p_d \neq 0$ and under the action of a bias, the MSD depends on p_x and p_y. The larger p_d is, the more the process is governed by the direction with larger concentration of bonds (p_x in this case). This becomes clearer when considering that although p_m is kept constant, increasing p_x causes a deformation of the cluster shape, the bonds connectivity in the x direction is increased, and the particle can diffuse easily in this direction. If we keep p_m constant and increase p_d, the trap becomes shallower in the direction of larger concentration of bonds, therefore B_c must increase due to the variation of p_d.

Using the same arguments, since the depth of the traps is decreased when p_m increases, it is expected that when p_d is kept constant and p_m increases, the value of B_c will increase too. This is actually the case shown in Fig. 3.

In Figs. 2(a), 2(c), and 2(d) we show that when keeping p_x constant and increasing p_y, the value of B_c increases (see also Fig. 5). This situation corresponds to a competition effect of increasing p_m (which increases B_c) and decreasing p_d (which decreases B_c). Then, since B_c increases although p_d decreases, it is clear that the effect of p_m is more important than that of p_d in order to change the depth of the trap in the relevant direction on anisotropic biased diffusion, at least for the small values of p_d as it is shown in these figures. In the inset of Fig. 3 we see that the effect of the anisotropy becomes more important when p_d approaches its maximum value p_d^*.

Finally, let us consider the behavior of the exponential parameter $A^{\text{ani}}(p_m, p_d)$ of Fig. 4. For high anisotropy, when the global occupancy increases, the A^{ani} versus p_m curves suddenly rise for $p_m \to p_m^*(p_d)$, indicating that the parameter $A^{\text{ani}}(p_m \to p_m^*, p_d) \to \infty$ and $B_c \to 1$. This means that the traps will disappear for $p_m \to p_m^*$.

C. Final conclusions

We have shown that there are two possible estimations of the critical bias for the drift/no-drift transition: from k_{eff} plots and from DS plots. In addition, these plots are useful for determining if one is in the $v \neq 0$ or $v = 0$ region of the phase diagram, like the one shown in Fig. 3.

We have shown a variety of phenomena related to the anisotropy of a disordered system, considering a particle which moves under the action of an external field. We have found that the direction of the bias is of great importance. For example, when we only have one disordered direction, the particle likely behaves as in the completely ordered case. This is so *because* the bias is in the diagonal direction and it can always push the RW. We have shown that the critical bias depends on the shape of the traps, i.e., deforming the traps causes a variation on B_c. Finally, we remark that the critical bias—for low and intermediate anisotropy—is more affected by the variation of the global occupancy of the system p_m than by the variation of the anisotropy parameter p_d. However, at higher anisotropies the critical bias is strongly affected by p_d as the system tends to a *quasiordered* behavior.

ACKNOWLEDGMENTS

S.B. acknowledges financial support from Secretaría de Investigación de la Universidad Nacional del Comahue. This work has been partially supported through grants from CONICET (No: 4948/96), and Secretaría de Investigación de la Universidad Nacional del Comahue.

[1] J. W. Haus and K. W. Kehr, Phys. Rep. **150**, 263 (1987); J. P. Bouchaud and A. Georges, *ibid.* **195**, 127 (1990).
[2] S. Havlin and D. Ben-Avraham, Adv. Phys. **36**, 695 (1987).
[3] J. P. de Gennes, Recherche **7**, 916 (1976).
[4] D. Stauffer and A. Aharony, in *Introduction to Percolation Theory* (Taylor & Francis, London, 1994).
[5] M. Sahimi, in *Applications of Percolation Theory* (Taylor & Francis, London, 1994); A. Bunde and S. Havlin, in *Fractals and Disordered Systems* (Springer, Berlin, 1996).
[6] H. Bottger and V. V. Bryskin, Phys. Status Solidi B **113**, 9 (1982).
[7] M. Barma and D. Dhar, J. Phys. C **16**, 1451 (1983).
[8] D. Dhar, J. Phys. A **17**, L257 (1984).
[9] R. B. Pandey, Phys. Rev. B **30**, 489 (1984).
[10] D. Stauffer, J. Phys. A **18**, 1827 (1985).
[11] D. Dhar and D. Stauffer, Int. J. Mod. Phys. C **9**, 349 (1998).
[12] A. Kirsch, Int. J. Mod. Phys. C **9**, 1021 (1998).
[13] D. Stauffer, Physica A **266**, 35 (1999).
[14] D. Stauffer and D. Sornette, Physica A **252**, 271 (1998).
[15] J. M. V. A. Koelman and A. de Kuijper, Physica A **247**, 10 (1997).
[16] A. Celzard, G. Furdin, J. F. Marêché, E. McRae, M. Dufort, and C. Deleuze, Solid State Commun. **92**, 377 (1994).
[17] E. R. Reyes, M. O. Cáceres, and P. A. Pury, Phys. Rev. B **61**, 308 (2000).
[18] G. Grimmet, *Percolation* (Springer-Verlag, Berlin, 1980).
[19] M. F. Sykes and J. W. Essam, Phys. Rev. Lett. **10**, 3 (1963).
[20] D. Sornette, Phys. Rep. **297**, 239 (1998).
[21] A. Kirsch, Int. J. Mod. Phys. C **10**, 753 (1999).